THE COMPANY OF
Biologists

RESEARCH ARTICLE

Pax9 regulates a molecular network involving Bmp4, Fgf10, Shh signaling and the Osr2 transcription factor to control palate morphogenesis

Jing Zhou[1], Yang Gao[2], Yu Lan[1], Shihai Jia[1] and Rulang Jiang[1,2,*]

ABSTRACT

Cleft palate is one of the most common birth defects in humans. Whereas gene knockout studies in mice have shown that both the Osr2 and Pax9 transcription factors are essential regulators of palatogenesis, little is known about the molecular mechanisms involving these transcription factors in palate development. We report here that Pax9 plays a crucial role in patterning the anterior-posterior axis and outgrowth of the developing palatal shelves. We found that tissue-specific deletion of *Pax9* in the palatal mesenchyme affected *Shh* expression in palatal epithelial cells, indicating that Pax9 plays a crucial role in the mesenchyme-epithelium interactions during palate development. We found that expression of the *Bmp4*, *Fgf10*, *Msx1* and *Osr2* genes is significantly downregulated in the developing palatal mesenchyme in *Pax9* mutant embryos. Remarkably, restoration of *Osr2* expression in the early palatal mesenchyme through a *Pax9^Osr2KI* allele rescued posterior palate morphogenesis in the absence of Pax9 protein function. Our data indicate that Pax9 regulates a molecular network involving the Bmp4, Fgf10, Shh and Osr2 pathways to control palatal shelf patterning and morphogenesis.

KEY WORDS: Cleft palate, Bmp4, Osr2, Pax9, Shh, Mouse

INTRODUCTION

The mammalian secondary palate initiates from the oral side of the maxillary processes as a pair of outgrowths that grow vertically down the sides of the developing tongue. At a precise developmental stage, the palatal shelves re-orient to the horizontal position above the dorsum of the tongue, and grow towards and subsequently fuse with each other at the midline. In addition, the palatal shelves fuse anteriorly with the primary palate, which is derived from the embryonic medial nasal processes, to form the intact roof of the oral cavity. Disturbances of the growth, elevation or fusion of the palatal shelves could result in cleft palate, one of the most common birth defects in humans (Bush and Jiang, 2012; Ferguson, 1988; Gritli-Linde, 2007).

The developing palatal shelves are composed of neural crest-derived mesenchyme (Ito et al., 2003) covered by a thin layer of oral epithelium, and exhibit distinct stereotyped shapes along the anterior-posterior (AP) axis (Bush and Jiang, 2012). Recent studies have demonstrated that many genes are differentially expressed along the AP axis in the developing palate (Baek et al., 2011;

[1]Cincinnati Children's Hospital Medical Center, Cincinnati, OH 45229, USA.
[2]Center for Oral Biology and Department of Biomedical Genetics, University of Rochester, Rochester, NY 14642, USA.

*Author for correspondence (rulang.jiang@cchmc.org)

Hilliard et al., 2005; Li and Ding, 2007; Liu et al., 2008; Welsh and O'Brien, 2009). For example, the short stature homeobox 2 (*Shox2*), Msh homeobox 1 (*Msx1*) and fibroblast growth factor 10 (*Fgf10*) genes are preferentially expressed in the anterior palatal mesenchyme (Alappat et al., 2005; Rice et al., 2004; Yu et al., 2005; Zhang et al., 2002), whereas the BarH-like homeobox 1 (*Barx1*), meningioma 1 (*Mn1*), mesenchyme homeobox 2 (*Meox2*) and T-box transcription factor 22 (*Tbx22*) genes are preferentially expressed in the posterior palatal mesenchyme (Barlow et al., 1999; Li and Ding, 2007; Liu et al., 2008), with the AP gene expression boundary coinciding with the first formed palatal ruga (Welsh and O'Brien, 2009). Moreover, anterior and posterior palatal mesenchyme cells exhibit distinct responses to epithelial signals. Exogenous Bmp4 induced *Msx1* mRNA expression in the anterior, but not posterior, palatal mesenchyme, whereas Fgf8 induced *Pax9* mRNA expression in the posterior, but not anterior, palatal mesenchyme (Hilliard et al., 2005). In addition, the anterior palatal epithelium has the unique ability to induce *Shox2* mRNA expression in the palatal mesenchyme (Yu et al., 2005). These data indicate that the developing palate is patterned along the AP axis by restricted gene expression in both the epithelium and mesenchyme.

Recent studies have shown that the anteriorward outgrowth of palatal shelves is associated with periodic formation of palatal rugae and is controlled by reciprocal epithelial-mesenchymal crosstalk along the AP axis (Lan and Jiang, 2009; Pantalacci et al., 2008; Welsh and O'Brien, 2009). The palatal rugae are the thickened epithelial ridges on the oral side of the secondary palate, and are formed in a defined sequence during palate outgrowth (Welsh and O'Brien, 2009). Palatal rugae express high levels of *Shh* and act as signaling centers involved in epithelial-mesenchymal interactions required to coordinate palate outgrowth and patterning (Lan and Jiang, 2009; Rice et al., 2006; Welsh and O'Brien, 2009). Shh from palatal epithelial cells stimulates cell proliferation and the expression of *Fgf10* in the developing palatal mesenchyme (Lan and Jiang, 2009), and Shh and Fgf10 function in a positive-feedback loop that drives the outgrowth of the palatal shelves (Bush and Jiang, 2012; Lan and Jiang, 2009; Rice et al., 2004). In addition, cross-regulation of the Shh and bone morphogenetic protein (Bmp) signaling pathways has also been detected in the developing palate (Baek et al., 2011; Lan and Jiang, 2009; Zhang et al., 2002).

We have reported previously that mice homozygous for a targeted null mutation in the *Osr2* gene had complete cleft palate (Lan et al., 2004). *Osr2* encodes a zinc-finger protein with extensive sequence similarity to the *Drosophila* Odd-skipped family transcription factors that regulate multiple developmental processes during embryogenesis and tissue morphogenesis (Coulter and Wieschaus, 1988; Green et al., 2002; Hao et al., 2003; Hart et al., 1996; Lan et al., 2001; Saulier-Le Dréan et al., 1998; Wang and Coulter, 1996). *Osr2*$^{-/-}$ mutant mice exhibited domain-specific defect in palatal
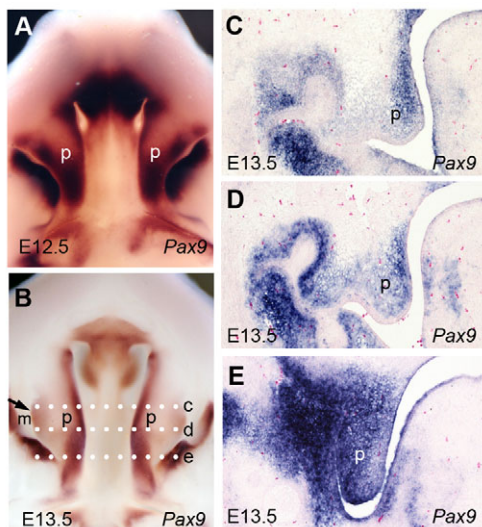
DEVELOPMENT

Fig. 1. *Pax9* mRNA expression during palate development. (A,B) Whole-mount *in situ* hybridization detection of *Pax9* mRNA in the developing palatal shelves in E12.5 (A) and E13.5 (B) mouse embryos. (C-E) Frontal sections through distinct planes along the anterior-posterior axis of the E13.5 palatal shelves showing *Pax9* mRNA expression pattern in the anterior (C), middle (D) and posterior (E) regions. Dotted white lines marked c-e in B indicate the section planes for C-E, respectively. m, molar tooth germ; p, palatal shelf.

mesenchyme cell proliferation and delay in palatal shelf elevation (Lan et al., 2004). In addition to cleft palate, $Osr2^{-/-}$ mutant mice developed supernumerary teeth lingual to their molar teeth (Zhang et al., 2009). *Osr2* mRNA expression exhibited a lingual-to-buccal gradient, complementary to that of *Bmp4*, in the mesenchyme surrounding the early developing tooth buds and patterns the tooth developmental field by suppressing the propagation of mesenchymal odontogenic activity driven by the Msx1-Bmp4 positive-feedback loop (Jia et al., 2013; Zhang et al., 2009).

Paired-box gene 9, also known as Pax9, is a member of the transcription factor family characterized by the Paired-class DNA-binding domain (Stapleton et al., 1993). *Pax9*-deficient mice die shortly after birth, exhibiting complete cleft palate (Peters et al., 1998). Little is known about the molecular and cellular mechanisms involving Pax9 in palate development, however. We recently generated a mouse strain ($Pax9^{fneo/+}$) that allows the Cre/loxP-mediated inactivation of the *Pax9* gene and subsequent activation of transgenic *Osr2* expression from the endogenous *Pax9* locus (Zhou et al., 2011). We report here that Pax9 is required for maintenance of *Osr2* expression in the developing palatal mesenchyme and that expression of *Osr2* from the *Pax9* locus partially rescued palate morphogenesis in *Pax9*-null mutant mice.

RESULTS

Pax9 exhibits differential expression patterns along the AP axis of the developing palate

To study the mechanism by which Pax9 regulates palate development, we first examined the expression patterns of Pax9 during palate development by whole-mount and section *in situ* hybridization. From E12.5 to E13.5, when the palate shelves grew vertically, *Pax9* exhibited a posterior-to-anterior gradient expression pattern in the palatal mesenchyme (Fig. 1A,B). Moreover, whereas *Pax9* mRNAs were expressed throughout the oral-nasal axis of the palatal mesenchyme in the posterior region (Fig. 1E), *Pax9* mRNA expression exhibited apparently lower levels in the oral half than in
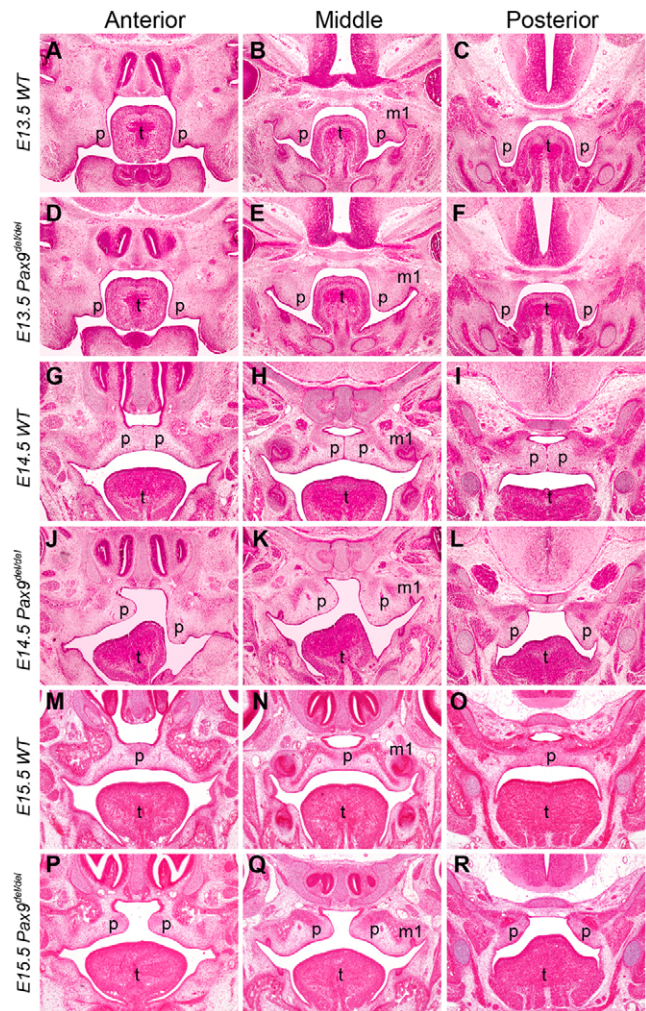

Fig. 2. Histological analysis of palate developmental defects in *Pax9^{del/del}* mutant mouse embryos. Representative frontal sections from the anterior, middle and posterior regions of the developing palatal shelves are shown. (A-F) E13.5 control (A-C) and mutant (D-F) littermates. (G-L) E14.5 control (G-I) and mutant (J-L) littermates. (M-R) E15.5 control (M-O) and mutant (P-R) littermates. m1, first molar tooth germ; p, palatal shelf; t, tongue.

the nasal half of the palatal mesenchyme in the anterior region (Fig. 1C,E).

Defects in palatal shape and AP patterning in *Pax9* mutant mice

We recently generated mice carrying a deletion of the first two exons of the *Pax9* gene ($Pax9^{del}$) and showed that $Pax9^{del/del}$ mutant mice displayed similar developmental defects, as reported previously in another *Pax9*-deficient mouse strain, including cleft palate and tooth developmental arrest (Peters et al., 1998; Zhou et al., 2011). Detailed histological analysis of $Pax9^{del/del}$ mutant embryos showed that the mutant palatal shelves had an aberrant shape and lacked the lateral indentation between the maxillary molar tooth germ and the palatal shelf at E13.5, in comparison with the wild-type littermates (Fig. 2A-F). At E14.5, the palatal shelves had elevated to the horizontal position above the developing tongue and initiated fusion at the midline in the control embryos (Fig. 2G-I). By contrast, the mutant embryos exhibited delay in palatal shelf elevation (Fig. 2J-L). By E15.5, the midline epithelial seam between
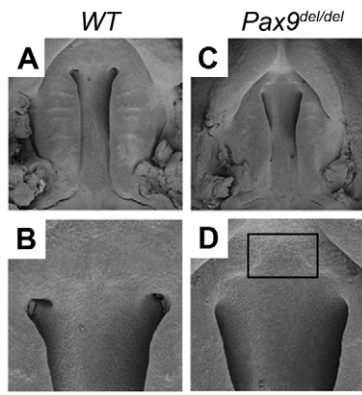
Fig. 3. Scanning electron microscopy analysis of palate developmental defects in *Pax9del/del* mutant mice. (A-D) Oral view of the developing palate in wild-type (A,B) and *Pax9del/del* mutant (C,D) embryos at E13.5. Rectangle in D marks the region of deficiency in primary palate.

the palatal shelves had mostly disappeared in the control embryos (Fig. 2M-O). By contrast, the mutant palatal shelves remained separate from each other (Fig. 2P-R). In addition to the lack of palatal fusion, scanning electron microscopy studies showed that the mutant palatal shelves had defects in formation of the palatal rugae, which are the thickened epithelial ridges on the oral side of the palatal shelves, and deficiency in primary palate outgrowth (Fig. 3A-D).

Recent studies showed that the palatal rugae express high levels of *Shh* mRNAs and are formed in a defined temporal sequence during palate outgrowth (Baek et al., 2011; Pantalacci et al., 2008; Welsh and O'Brien, 2009). Our whole-mount *in situ* hybridization analyses confirmed that the *Pax9del/del* mutant embryos had defects in palatal rugae formation. At E12.0, when two pairs of clearly defined rugae had formed in wild-type embryos (Fig. 4A), the *Pax9del/del* mutant embryos showed diffuse *Shh* mRNA expression in the palatal epithelium and lacked clearly demarcated rugae structures (Fig. 4E). From E12.5 to E14.5, the palatal rugae formed sequentially in a defined sequence as the palatal shelves grew rostrally (Fig. 4B-D). In the mutant palate, although two pairs of strong *Shh*-expressing rugae were detected in the anterior most region, corresponding to R2 and R3 in the control palate, *Shh*

expression was much weaker and not distinctly localized in discrete rugae structures in the middle region of the palatal shelves at E13.5 in the mutant embryos (Fig. 4G). By E14.5, the *Shh*-expressing rugae structures were better demarcated but there were fewer rugae and the distance between R1 and R5 was significantly shorter in the mutant embryos than in the control littermates (compare Fig. 4D with 4H), indicating impairment in anteriorward outgrowth of the palatal shelves in the mutant embryos. In addition, the punctate *Shh* expression pattern observed in the developing sensory papilla overlying the posterior soft palate was absent in the *Pax9del/del* mutant embryos (Fig. 4D,H). The mutant embryos also exhibited reduced *Shh* expression in the primary palate, in comparison with the control littermates (Fig. 4D,H).

Pax9 was expressed in the palatal mesenchyme, as well as in the posterior palatal epithelium (Fig. 1). To investigate whether defects in *Shh* expression were due to loss of Pax9 function in the epithelium, we inactivated *Pax9* specifically in neural crest-derived mesenchymal cells by crossing the *Pax9fneo* mice with *Wnt1-Cre* transgenic mice (Danielian et al., 1998). We found that the *Pax9fneo/del*;*Wnt1-Cre* mutant embryos showed similar defects in *Shh* mRNA expression to the *Pax9del/del* mutant embryos in both the primary and secondary palate (compare Fig. 5 with Fig. 4). These results suggest that Pax9 plays an important role in regulating the mesenchymal-epithelial interactions during palate development.

In addition to defects in the anteriorward outgrowth of the palate shelves, we found that the anterior-posterior boundary of the palatal mesenchyme was disturbed in the *Pax9del/del* mutant embryos. As shown in Fig. 6, expression of *Shox2* was restricted anterior to R1, whereas *Barx1* expression was restricted posterior to R1 in the E13.5 wild-type palate (Fig. 6A,C). By contrast, both the posterior boundary of *Shox2* expression and the anterior boundary of *Barx1* expression appeared diffuse and anteriorly shifted in the *Pax9del/del* mutant palate (Fig. 6B,D). Taken together, these results indicate that deletion of *Pax9* resulted in disruption of the AP boundary of the palatal mesenchyme, which correlated with the misshapen palatal shelves and defects in expansion of the palatal shelves along the AP axis in the *Pax9del/del* mutant embryos.

Pax9 acts upstream of Bmp4, Fgf10, Msx1 and Osr2 in the palatal mesenchyme

The defects in *Shh* expression in the palatal epithelium in both the *Pax9del/del* and *Pax9fneo/del*;*Wnt1-Cre* mouse embryos indicate that
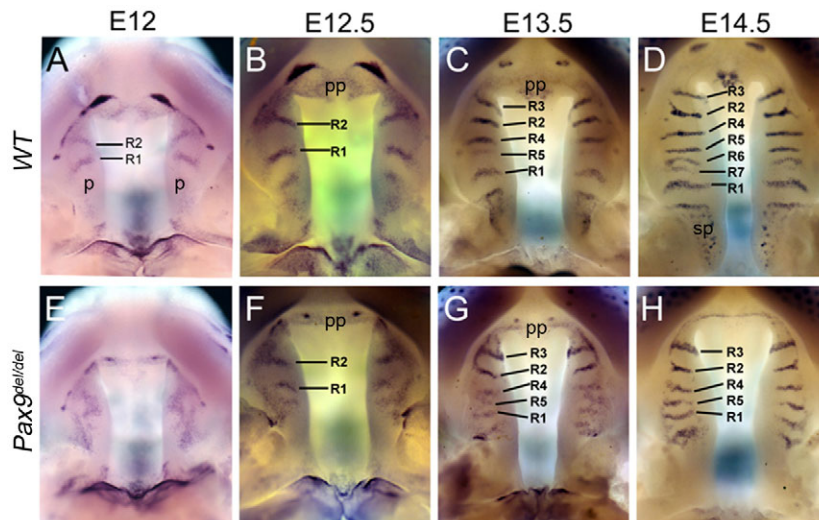

Fig. 4. Analysis of palatal ruga formation and anteriorward palatal outgrowth in *Pax9del/del* mutant embryos. (A-H) Whole-mount *in situ* hybridization detection of patterns of *Shh* mRNA expression in the developing palate in wild-type control (A-D) and *Pax9del/del* mutant (E-H) embryos from E12.0 to E14.5. Strong *Shh* mRNA expression marks the palatal rugae, which increase in number from two at E12.0 to seven pairs by E14.5 in the wild-type embryos (A-D), whereas the mutant had formed only five pairs by E14.5 (E-H). p, palatal shelf; pp, primary palate; sp, sensory papilla.
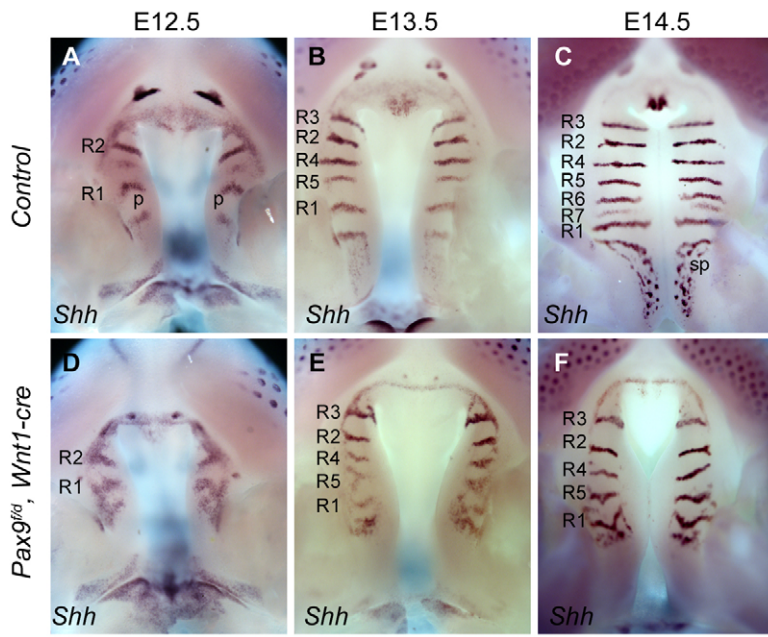
Fig. 5. Palatal *Shh* mRNA expression pattern in *Pax9^fneo/del*;*Wnt1Cre* mutant embryos. (A-F) Patterns of *Shh* mRNA expression in the palate in wild-type (A-C) and *Pax9^fneo/del*;*Wnt1-Cre* mutant (D-F) embryos from E12.5 to E14.5. p, palatal shelf; sp, sensory papilla.

Pax9 regulates mesenchymal-epithelial crosstalk during palate development. To investigate the molecular mechanism that mediates Pax9 function in palate development, we carried out extensive molecular marker analyses by using both quantitative real-time RT-PCR and *in situ* hybridization analyses of E12.5 and E13.5 embryos. Expression of *Bmp4* and *Msx1* mRNAs were consistently significantly reduced in the *Pax9^del/del* mutant palate (Fig. 7A,B).

Whereas previous studies using section *in situ* hybridization analysis suggested that expression of both *Msx1* and *Bmp4* was restricted in the anterior palate (Zhang et al., 2002), our whole-mount *in situ* hybridization assays demonstrated that, although *Msx1* mRNA expression was restricted in the anterior palate (Fig. 8A-D), the *Bmp4* mRNA expression pattern in the developing palatal shelves consisted of an anterior and a posterior domain separated by a *Bmp4*-negative middle palatal region (Fig. 8E,G). We further confirmed this unique pattern of *Bmp4* mRNA expression by section *in situ* hybridization of the whole series of frontal sections through the developing palatal
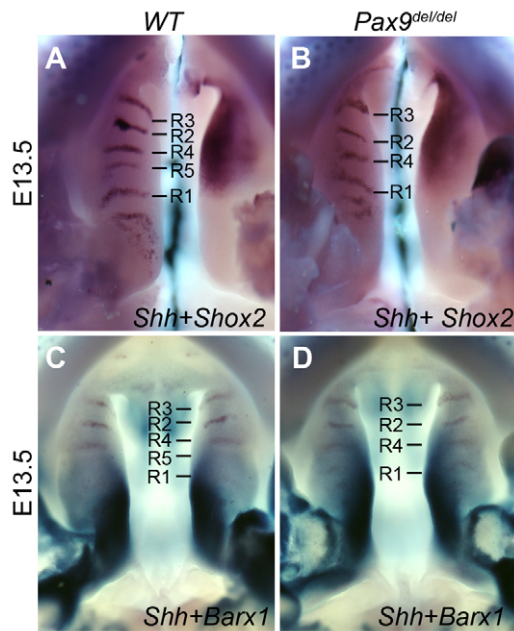

Fig. 6. Disruption of the anterior-posterior boundary in the secondary palate in *Pax9^del/del* mutant embryos. (A,B) Direct comparison of *Shh* (left half) and *Shox2* (right half) mRNA expression patterns in the palatal shelf pairs in wild-type (A) and *Pax9^del/del* mutant (B) embryos at E13.5. (C,D) Dual color *in situ* hybridization detection of *Shh* (brown) and *Barx1* (turquoise) mRNAs in the palatal shelves of E13.5 wild-type (C) and *Pax9^del/del* mutant (D) embryos.
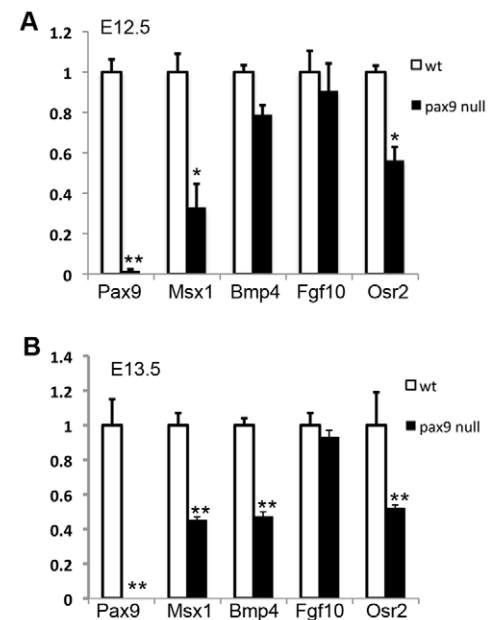
Fig. 7. Quantitative RT-PCR analysis of the levels of expression of *Pax9*, *Msx1*, *Bmp4*, *Fgf10* and *Osr2* mRNAs in E12.5 and E13.5 palatal shelves in wild-type and *Pax9^del/del* mutant embryos. (A) E12.5, (B) E13.5. Error bars represent s.e.m. *$P<0.05$; **$P<0.01$.
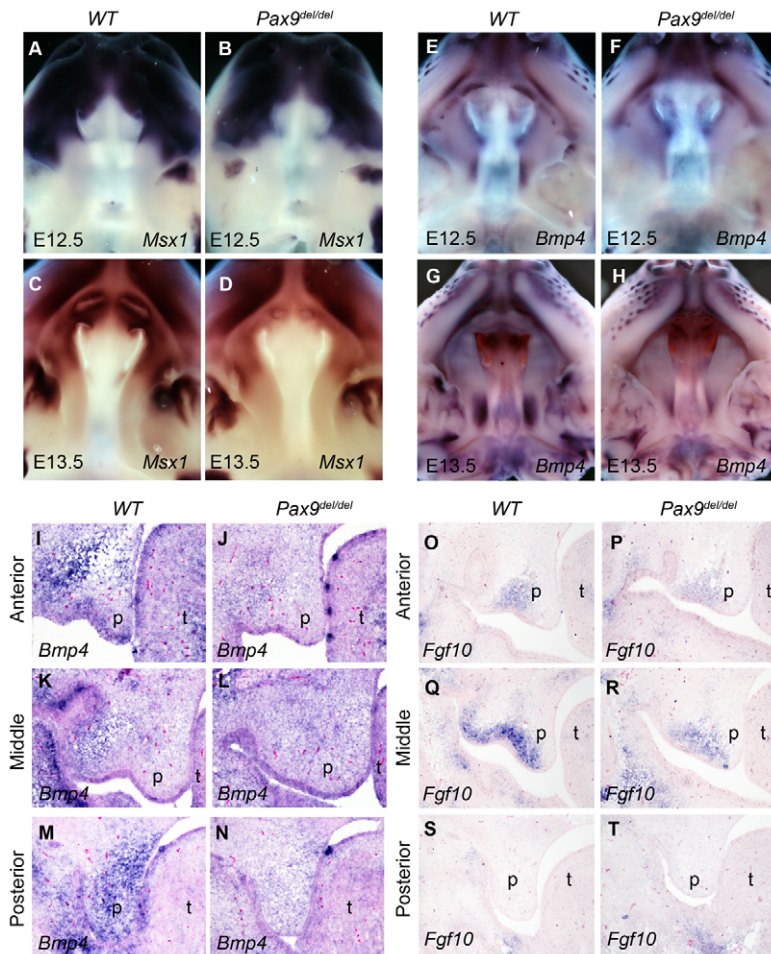
Fig. 8. Comparison of expression of *Bmp4*, *Fgf10* and *Msx1* mRNAs in the palatal shelves in *Pax9del/del* mutant and control embryos. (A-D) Whole-mount *in situ* hybridization results of *Msx1* mRNA expression in wild-type (A,C) and *Pax9del/del* mutant (B,D) embryos at E12.5 (A,B) and E13.5 (C,D). (E-H) Whole-mount *in situ* hybridization results of *Bmp4* mRNA expression in wild-type (E,G) and *Pax9del/del* mutant (F,H) embryos at E12.5 (E,F) and E13.5 (G,H). (I-N) Frontal sections showing expression of *Bmp4* mRNAs in the anterior, middle and posterior regions of the developing palate in E13.5 wild-type (I,K,M) and *Pax9del/del* mutant (J,L,N) embryos. (O-T) Frontal sections showing expression of *Fgf10* mRNA in the anterior, middle and posterior regions of the developing palate in E13.5 wild-type (O,Q,S) and *Pax9del/del* mutant (P,R,T) embryos. p, palatal shelf; t, tongue.

shelves of E13.5 mouse embryos and found that expression of *Bmp4* mRNAs was significantly reduced in both the anterior and posterior regions of the developing palate of *Pax9del/del* mutant embryos in comparison with control littermates (Fig. 8E-N).

Our real-time RT-PCR analyses also consistently detected a reduction in the amount of *Fgf10* mRNAs in the microdissected E12.5 and E13.5 mutant palatal tissues in comparison with the control samples, although the difference was not statistically significant (Fig. 7A,B). This was probably due to the overall low abundance and highly restricted domain of *Fgf10* mRNA expression in the developing palatal shelves, as *Fgf10* mRNA expression was restricted to only the anterior and middle oral quarters of the developing palatal mesenchyme (Fig. 8O,Q,S). Indeed, section *in situ* hybridization assays consistently showed reduced *Fgf10* mRNA expression in the *Pax9del/del* mutant palate in comparison with control littermates (Fig. 8O-T).

We have previously shown that Pax9 is required for maintenance of *Osr2* mRNA expression in the developing tooth mesenchyme (Zhou et al., 2011). In this study, we found that *Osr2* mRNA expression was significantly reduced in the developing palate in the *Pax9del/del* mutant embryos, as detected by both real-time RT-PCR and whole-mount *in situ* hybridization assays (Fig. 7A,B; Fig. 9A,B). We further verified the changes in *Osr2* mRNA expression by using section *in situ* hybridization assay and found that *Osr2* mRNA expression was dramatically reduced in the middle and posterior regions of the palatal shelves, whereas a higher level of *Osr2* mRNA expression was present in the very anterior region of the mutant

palatal mesenchyme at E13.5 (Fig. 9C-H). Moreover, we found that expression of *Fgf10* mRNAs was also downregulated in the developing palatal shelves in *Osr2−/−* mutant embryos, in comparison with wild-type littermates (Fig. 9I-L). Together, these results suggest that Osr2 might act downstream of Pax9 to maintain *Fgf10* expression in the palatal mesenchyme during palatal outgrowth.

Expression of Osr2 from the *Pax9* locus rescued posterior palate morphogenesis in *Pax9*-deficient mice

To further investigate the role of Osr2 in Pax9-mediated regulation of palate development, we examined palatogenesis in the *Pax9Osr2KI/Osr2KI* mice, in which an *Osr2* cDNA replaced the first two exons of the endogenous *Pax9* gene (Zhou et al., 2011). Whereas *Pax9del/del* mutant newborn pups had complete cleft secondary palate (Fig. 10B), 50% of the *Pax9Osr2KI/Osr2KI* newborn pups exhibited fused posterior secondary palate, with a partial cleft in the anterior palate region only (*n*=24) (Fig. 10C). Histological analyses of E14.5 embryos showed that the *Pax9Osr2KI/Osr2KI* mutant embryos exhibited rescue of the defects in palatal shelf elevation (*n*=4), in comparison with the *Pax9del/del* mutant embryos that always showed defects in palatal shelf elevation (Fig. 10D-F). By E16.5, 50% of the *Pax9Osr2KI/Osr2KI* mutant embryos showed a fused posterior palate (*n*=6) (Fig. 10L), but the anterior region of the palate shelves failed to make contact at the midline (Fig. 10I).

Osr2 plays an important role in regulating palatal mesenchyme cell proliferation (Lan et al., 2004). We analyzed palatal cell proliferation in *Pax9del/del* embryos and control littermates by using
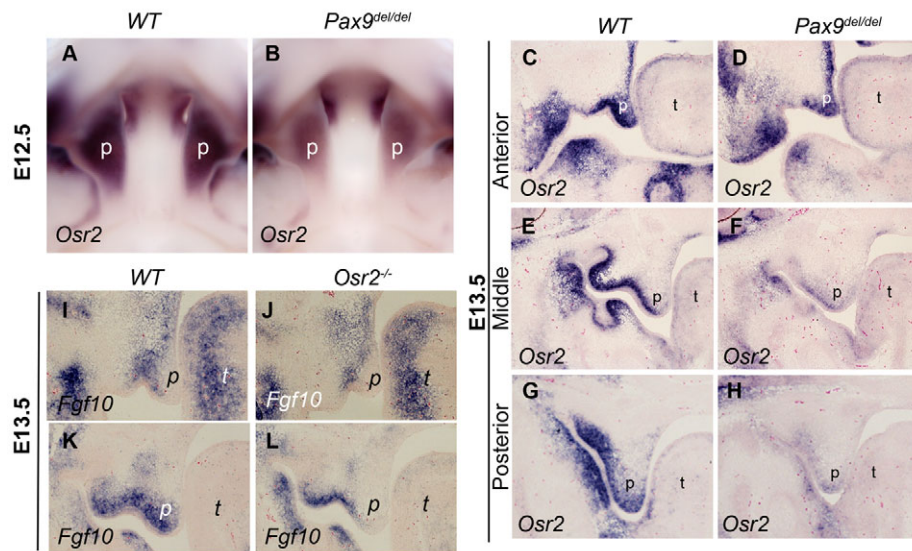
Fig. 9. Pax9 is required to maintain *Osr2* mRNA expression in the developing palatal shelves. (A,B) Whole-mount *in situ* hybridization results of *Osr2* mRNA expression in the palatal shelves in E12.5 wild-type control (A) and *Pax9* mutant (B) littermates. (C-H) Frontal sections showing *Osr2* mRNA expression in the anterior (C,D), middle (E,F) and posterior (G,H) regions of the developing palatal shelves in E13.5 wild-type (C,E,G) and *Pax9del/del* mutant (D,F,H) embryos. (I-L) Frontal sections showing *Fgf10* mRNA expression in the anterior (I,J) and middle (K,L) regions of the developing palatal shelves in E13.5 wild-type (I,K) and *Osr2−/−* mutant (J,L) embryos . p, palatal shelf; t, tongue.

BrdU labeling and found that the posterior palate region, but not the anterior palate region, had significant reduction in cell proliferation in E13.5 *Pax9del/del* embryos in comparison with their control littermates (Fig. 11A-D; Fig. 11I). This posterior palatal growth defect was rescued in the *Pax9Osr2KI/Osr2KI* embryos (Fig. 11E-I), confirming a crucial role for Osr2 in palatal shelf growth and indicating that the reduction in palatal growth contributed to cleft palate pathogenesis in the *Pax9del/del* mice.

We investigated further whether the rescued morphogenesis of the posterior palate in the *Pax9Osr2KI/Osr2KI* mutant embryos correlated with restoration of *Bmp4, Msx1, Shh* and *Fgf10* mRNA expression during palate development. We examined more than four pairs of
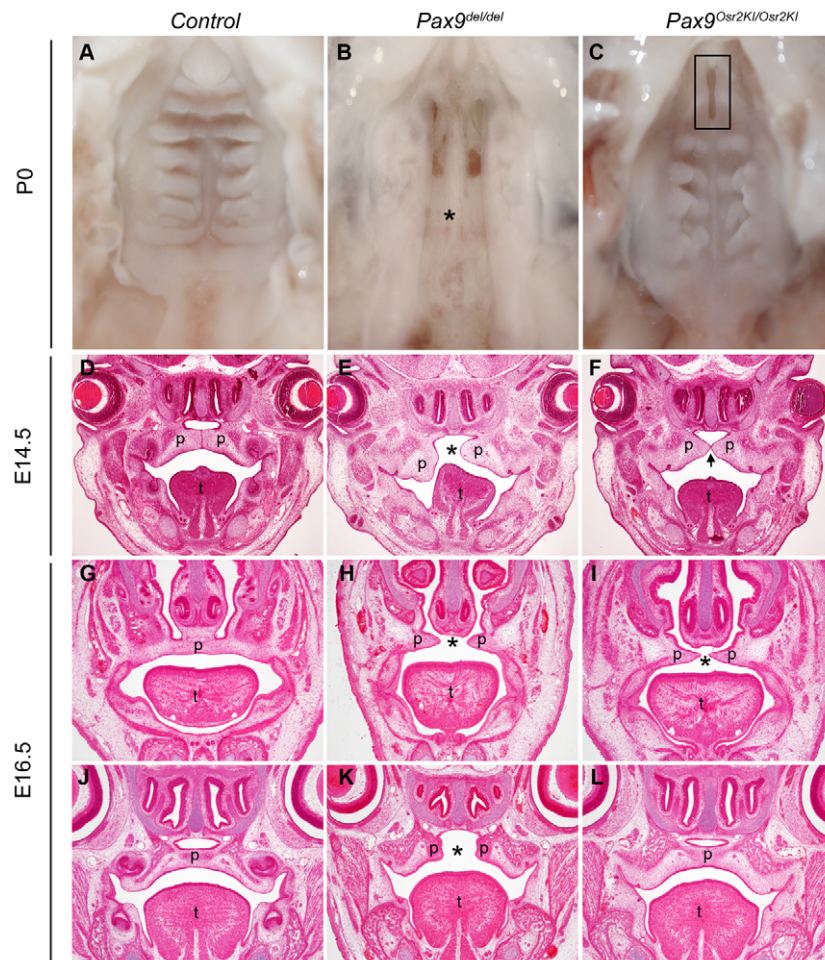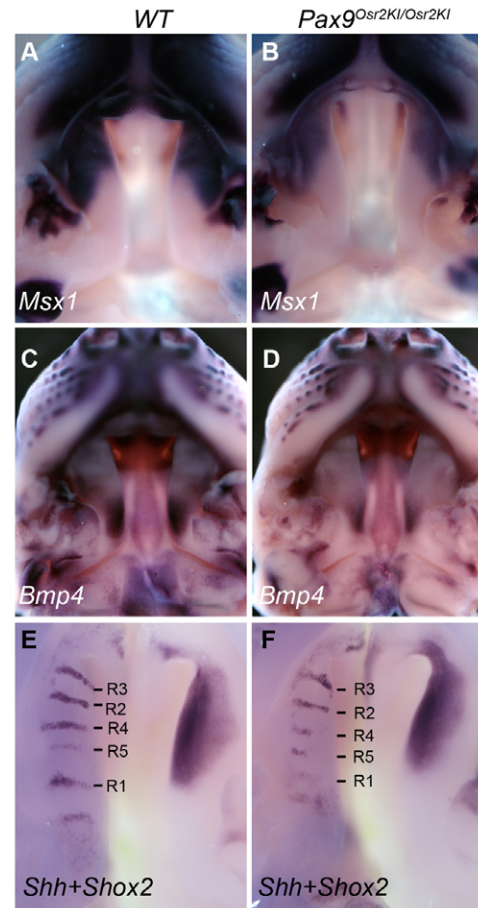

Fig. 10. Partial rescue of palate morphogenesis in the *Pax9Osr2KI/Osr2KI* mutant mice. (A-C) Oral view of the palate in control (A), *Pax9del/del* mutant (B) and *Pax9Osr2KI/Osr2KI* mutant (C) newborn pups. In contrast to complete cleft secondary palate in the *Pax9del/del* mutant (asterisk in B), *Pax9Osr2KI/Osr2KI* mutant pups had a partial cleft of the anterior palate (rectangle in C). (D-F) Histology of frontal sections through the middle regions of the developing palate in E14.5 control (D), *Pax9del/del* mutant (E) and *Pax9Osr2KI/Osr2KI* mutant (F) embryos. Arrow in F indicates the midline epithelial seam of the palatal shelves. (G-L) Frontal sections through the anterior (G-I) and posterior (J-L) regions of the developing palate in E16.5 control (G,J), *Pax9del/del* mutant (H,K) and *Pax9Osr2KI/Osr2KI* mutant (I,L) embryos. Asterisk indicates the gap between the palatal shelves. p, palatal shelf; t, tongue.
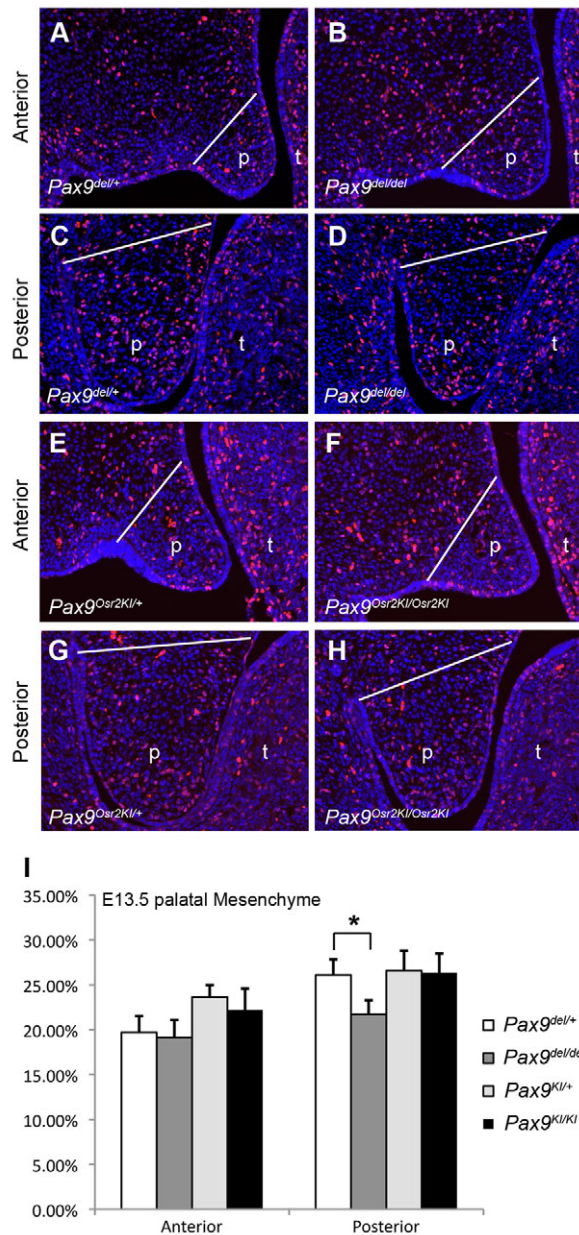
Fig. 11. Analysis of cell proliferation in the developing palate in E13.5 *Pax9^del/del* and *Pax9^Osr2KI/Osr2KI* embryos. (A-D) Representative images of sections through the anterior (A,B) and posterior (C,D) regions of the palate in *Pax9^del/+* control (A,C) and *Pax9^del/del* mutant (B,D) embryos showing distribution of immunostained BrdU-labeled nuclei (red). Sections were counterstained with Hoechst (blue). (E-H) Representative images of sections through the anterior (E,F) and posterior (G,H) regions of the palate in *Pax9^Osr2KI/+* (E,G) and *Pax9^Osr2KI/Osr2KI* mutant (F,H) embryos showing distribution of immunostained BrdU-labeled nuclei (red). White line indicates approximate position below which the palatal mesenchyme cells were counted. (I) The percentage of BrdU-labeled cells in the E13.5 palatal mesenchyme. Error bar represents s.d. *$P<0.01$.

Fig. 12. Comparison of patterns of expression of *Msx1*, *Bmp4*, *Shh* and *Shox2* mRNAs in E13.5 wild-type and *Pax9^Osr2KI/Osr2KI* mutant palate. (A,B) Whole-mount view of *Msx1* mRNA expression in the palate in control (A) and *Pax9^Osr2KI/Osr2KI* mutant (B) embryos. (C,D) Whole-mount view of *Bmp4* mRNA expression in the palate in control (C) and *Pax9^Osr2KI/Osr2KI* mutant (D) embryos. (E,F) Whole-mount *in situ* hybridization results for *Shh* (left half) and *Shox2* (right half) mRNA expression in bisected upper jaw samples of control (E) and *Pax9^Osr2KI/Osr2KI* mutant (F) embryos. R1 to R5 mark the rugae according to the temporal sequence of formation.

E13.5 embryos for each probe and all *Pax9^Osr2KI/Osr2KI* mutant embryos exhibited reduced expression of *Msx1* and *Bmp4* mRNAs in the developing palatal shelves, in comparison with the wild-type littermates (Fig. 12A-D). Moreover, the *Pax9^Osr2KI/Osr2KI* mutant embryos showed loss of *Shh* mRNA expression in the posterior palate and decreased *Shh* mRNA expression in the rugae in the mid-palate region, similar to the *Pax9^del/del* mutant embryos (compare Fig. 12E,F and Fig. 4C,G). The domain of *Shox2* mRNA expression in the palatal shelves was also similarly shifted anteriorly in the *Pax9^Osr2KI/Osr2KI* embryos as in the *Pax9^del/del* mutant embryos (compare Fig. 12E,F and Fig. 6A,B). However, we found that two out of five *Pax9^Osr2KI/Osr2KI* mutant embryos had restored *Fgf10* mRNA expression in the anterior and middle palate regions at E13.5 (Fig. 13A-D). Together, these results suggest that Osr2 acts downstream of or in parallel with the Bmp4 and Shh pathways and cooperates with Pax9 to maintain *Fgf10* expression during palate development.

DISCUSSION

Although cleft palate in *Pax9*-deficient mice was first reported more than 15 years ago (Peters et al., 1998), the molecular mechanisms involving Pax9 in palate development have not been documented. In this study, we found that Pax9 regulates mesenchymal-epithelial signaling and AP patterning during palate outgrowth and that Pax9 acts upstream of Osr2 to regulate palatal shelf growth and elevation.
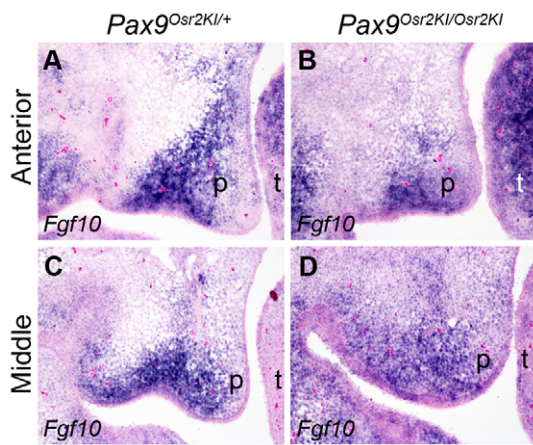
Fig. 13. Comparison of Fgf10 mRNA expression in the developing palate in E13.5 control and *Pax9$^{Osr2KI/Osr2KI}$* mutant embryos. (A-D) Representative frontal sections through the anterior (A,B) and middle (C,D) regions of the developing palatal shelves were used for detection of *Fgf10* mRNA expression by section *in situ* hybridization. p, palatal shelf; t, tongue.

Reciprocal signaling between the epithelium and neural crest derived mesenchyme plays a crucial role in the growth of the secondary palate (Bush and Jiang, 2012; Lan and Jiang, 2009; Rice et al., 2004; Welsh and O'Brien, 2009). We found that disruption of patterns of *Shh* expression in the palatal epithelium was among the earliest detectable defects during palate development in the *Pax9$^{del/del}$* mutant mice. Remarkably, *Shh* mRNA expression in the palatal epithelium was also disrupted in the *Pax9$^{fNeo/del}$Wnt1-Cre* mutant embryos (Fig. 5), indicating that Pax9-mediated transcriptional regulation in the neural crest-derived palatal mesenchyme indirectly regulates *Shh* expression in the palatal epithelium. Previous studies of cleft palate pathogenesis in the *Msx1$^{-/-}$* mutant mice implicated a role for Bmp4 acting downstream of Msx1 in the palatal mesenchyme but upstream of *Shh* expression in the palatal epithelium in the anterior palate (Zhang et al., 2002). Whereas Zhang et al. (Zhang et al., 2002), using only the section *in situ* hybridization assay, suggested that expression of both *Msx1* and *Bmp4* was restricted to the anterior palate region, our whole-mount *in situ* hybridization assays clearly detected strong *Bmp4* mRNA expression in a discrete domain in the posterior palate at both E12.5 and E13.5 (Fig. 8E,G). Levi et al. (Levi et al., 2006) reported whole-mount *in situ* hybridization results for *Bmp4* mRNA expression in the E13.5 palate and also clearly showed a strong *Bmp4* expression domain in the posterior palate (Levi et al., 2006). We carried out section *in situ* hybridization of the whole series of frontal sections of E13.5 mouse palate and confirmed the separate *Bmp4* mRNA expression domains in the anterior and posterior regions of the palatal shelves (Fig. 8I,K,M). Moreover, Levi et al. (Levi et al., 2006) showed that *Bmp4* mRNA expression in the anterior palate, but not in the posterior palate, was reduced in the *Msx1$^{-/-}$* embryos in comparison with wild-type control embryos (Levi et al., 2006). We found that the posterior domain of *Bmp4* mRNA expression was significantly downregulated in the *Pax9$^{del/del}$* mutant embryos, indicating that Pax9 regulates *Bmp4* expression in the posterior palate independently of Msx1. Previous biochemical studies have shown that Pax9 could activate the luciferase reporter expression driven by either the *Msx1* or *Bmp4* gene promoter in co-transfected COS7 cells (Ogawa et al., 2006). Together, these data suggest that Pax9 directly regulates both *Msx1* and *Bmp4* expression in the

palatal mesenchyme and that *Bmp4* expression in the posterior palate may also be involved in maintenance of *Shh* expression in the palatal epithelium.

In addition to Bmp4, mesenchymally expressed Fgf10 is involved in maintenance of *Shh* expression in the palatal epithelium, with Fgf10 and Shh acting in a positive-feedback loop to regulate palatal outgrowth (Lan and Jiang, 2009; Rice et al., 2004). *Fgf10* mRNA expression was downregulated in the *Pax9$^{del/del}$* mutant palatal shelves. Interestingly, we found that *Fgf10* mRNA expression was also downregulated in the *Osr2$^{-/-}$* mutant palatal shelves and that *Osr2* mRNA expression was significantly downregulated in *Pax9$^{del/del}$* mutant palatal shelves. Moreover, we found that *Fgf10* mRNA expression was restored in a subset of *Pax9$^{Osr2KI/Osr2KI}$* mutant palate, which correlated with partial rescue of palate morphogenesis in the *Pax9$^{Osr2KI/Osr2KI}$* mutant embryos. Together, these data suggest that Pax9 may regulate *Fgf10* expression in the developing palatal mesenchyme through Osr2.

Whereas *Osr2$^{-/-}$* and *Pax9$^{del/del}$* mutant mice each had cleft palate, the palatal phenotypes were not the same. *Osr2$^{-/-}$* mutant embryos had reduced mesenchyme cell proliferation throughout the AP axis of the palatal shelves at E13.5 (Lan et al., 2004), whereas *Pax9$^{del/del}$* mutant embryos showed reduced mesenchymal cell proliferation only in the posterior region and exhibited malformed palatal shelves lacking the lateral indentation. However, both *Osr2$^{-/-}$* and *Pax9$^{del/del}$* mutant embryos had defects in palatal shelf elevation (Lan et al., 2004; and this study). We found that *Osr2* mRNA expression was significantly downregulated in *Pax9$^{del/del}$* mutant palatal shelves as early as E12.5 and that restoration of *Osr2* expression in the palatal mesenchyme through the *Pax9^{Osr2KI}* allele rescued palatal elevation and posterior palate morphogenesis in ~50% of the *Pax9$^{Osr2KI/Osr2KI}$* mutant mice (Fig. 10). Whether *Osr2* is a direct target of Pax9 transcriptional regulation requires further investigation, however, because maintenance of *Osr2* mRNA expression in the developing palatal shelves requires active Shh signaling (Lan and Jiang, 2009) but *Shh* expression was significantly perturbed in the *Pax9$^{del/del}$* mutant palate. Moreover, although posterior palate morphogenesis was rescued in the *Pax9$^{Osr2KI/Osr2KI}$* embryos in comparison with *Pax9$^{del/del}$* mutants, the restoration of Osr2 to the palatal mesenchyme through the *Pax9^{Osr2KI}* allele was insufficient to rescue the effects of loss of Pax9 on expression of *Bmp4*, *Msx1* and *Shh* in the developing palate. Furthermore, we found that *Osr2* mRNA expression was more dramatically reduced in the middle and posterior regions of the *Pax9$^{del/del}$* mutant palate, which correlated with the reduced expression of *Shh* mRNA expression in the middle and posterior regions of the palatal epithelium in these mutant embryos. Together, these results suggest that Pax9 plays a primary role in regulating the mesenchymal-epithelial interactions involving the Bmp4 and Shh signaling, and that Osr2 acts downstream of these pathways to regulate palatal cell proliferation and palatal shelf elevation.

Defects in palatal shelf elevation have been attributed to malformation of or physical obstruction by the tongue in several mutant mouse strains (Barrow et al., 2000; Dudas et al., 2004; Gendron-Maguire et al., 1993; Murray et al., 2007; Wang et al., 2003). In the *Pax9$^{del/del}$* mutant embryos, failure of palatal shelf elevation was also accompanied by abnormal morphology of the tongue (Fig. 2K,L,R). However, we found that *Pax9$^{del/del}$* mutant embryos had defects in expression of *Shh*, *Msx1* and *Bmp4* by E12.5, and exhibited abnormally broadened mid-palate region by E13.5, indicating that the mutant palatal shelves were already malformed 1 day before the time of normal palatal shelf elevation. The abnormal broadening of the palatal shelves in the mid-palate region correlated with the disruption

of the anterior-posterior boundary of the palatal shelves, whereas the lack of indentation lateral to the palatal shelves correlated with the early developmental arrest of the molar tooth germs in the mutant embryos. As all $Pax9^{Osr2KI/Osr2KI}$ embryos also had early developmental arrest of the molar tooth germs (Zhou et al., 2011), but about half of those mutants developed fused posterior secondary palate (Fig. 10L), the tooth developmental defect was unlikely to be a determining factor in palatal shelf elevation. However, we found that some, but not all, of the $Pax9^{Osr2KI/Osr2KI}$ embryos had restored $Fgf10$ mRNA expression in the palatal mesenchyme, which correlated with partial rescue of palate morphogenesis in those mutants. Thus, although we have not ruled out possible contribution by abnormalities of surrounding structures, including the tooth germs and tongue, to the impairment of palatal shelf elevation in the $Pax9^{del/del}$ mutant embryos, our data support a crucial role for Pax9-dependent gene expression within the developing palatal shelves in palatal shelf elevation.

Whereas 50% of late-term $Pax9^{Osr2KI/Osr2KI}$ embryos showed fusion of the posterior palate, all of the mutant embryos had cleft of the anterior palate. The anterior cleft palate defect correlated with the reduction in $Msx1$ expression in the anterior palate in both $Pax9^{del/del}$ and $Pax9^{Osr2KI/Osr2KI}$ embryos (Fig. 12C,D). As $Msx1$ is not expressed in the posterior palate, these results indicate that Pax9 regulates palate development through distinct molecular pathways in the anterior and posterior regions. Similar to the anterior palatal mesenchyme, the developing tooth bud mesenchyme exhibits partially overlapping expression of $Msx1$, $Pax9$ and $Osr2$ (Zhang et al., 2009; Zhou et al., 2011). We recently discovered that Msx1 and Osr2 interact physically but act antagonistically in the regulation of mesenchymal odontogenic activity (Jia et al., 2013; Zhang et al., 2009; Zhou et al., 2011). It is possible that the Msx1-Osr2 interaction may play an important role in the development of the anterior palate. In the $Pax9^{Osr2KI/Osr2KI}$ embryos, the reduction of $Msx1$ expression affects the pathways downstream of Msx1-Osr2 interactions, which would account for the anterior cleft palate defect. Together, these results indicate that both Osr2 and Pax9 interact with the distinct molecular pathways in the anterior and posterior palate. The $Pax9^{Osr2KI/Osr2KI}$ mutant mice provide a valuable tool for comprehensive analysis of the gene regulatory network controlling palate development and patterning.

MATERIALS AND METHODS
Mouse strains
$Pax9^{fneo/+}$, $Pax9^{del/+}$ and $Pax9^{Osr2KI/+}$ mice have been described previously (Zhou et al., 2011). $Pax9^{del/+}$ and $Pax9^{Osr2KI/+}$ mice were maintained in the C57BL/6J strain background and were intercrossed to generate homozygous mutants for analyses. $Pax9^{fneo/+}$ mice were crossed with $Wnt1$-Cre transgenic mice (Danielian et al., 1998) to generate $Pax9^{fneo/+}Wnt1$-Cre mice, which were then crossed with $Pax9^{del/+}$ mice to generate $Pax9^{fneo/del}Wnt1$-Cre mutant embryos for analyses.

Scanning electron microscopy
Embryos were fixed with 2% glutaraldehyde/2% paraformaldehyde in PBS followed by OsO_4 treatment and dehydration through an ethanol series. The embryos were critical point dried under CO_2 and sputter coated with 30 nm gold particles. Images were obtained using Zeiss Supra 40VP Field Emission at the Electron Microscope Research Core of the University of Rochester Medical Center (NY, USA).

Histology and *in situ* hybridization
Embryos were collected at desired developmental stages and fixed in 4% paraformaldehyde overnight at 4°C. For whole-mount *in situ* hybridization, embryos were dehydrated through graded methanol. For section *in situ* hybridization, embryos were dehydrated through graded alcohols, embedded

in paraffin and sectioned at 7 μm. Whole-mount (Baek et al., 2011; Lan et al., 2001) and section *in situ* hybridization (Zhang et al., 1999) were carried out as described previously with digoxygenin or fluorescein-labeled antisense RNA probes. For section *in situ* hybridization, frontal sections through palatal shelves were selected from the anterior, middle and posterior regions, with the middle region consisting of sections through the maxillary first molar tooth buds.

For histology, embryos were fixed in either Bouin's fixative or 4% paraformaldehyde. Fixed embryos were dehydrated through a graded series of ethanol and embedded in paraffin wax. Serial sections of 7 μm were stained with Hematoxylin and Eosin.

BrdU labeling and cell proliferation assay
For detection of cell proliferation in the palatal shelves, timed-mated pregnant female mice were injected once intraperitoneally at gestational day 13.5 with the BrdU Labeling Reagent (Roche, 15 μl/g body weight). One hour after injection, embryos were dissected, fixed in 4% paraformaldehyde at 4°C overnight, embedded in paraffin wax and sectioned at 5 μm in the coronal plane. The sections were rehydrated and submerged in pre-cooled acetone at −20°C for 30 minutes. After washing with PBS, the specimens were treated with 20 μg/ml proteinase K at room temperature for 10 minutes. After washing with PBS, sections were treated with 2 M HCl for 1 hour at room temperature to denature the genomic DNA. Samples were rinsed in PBS for three times, then incubated in blocking solution (2% BSA, 10% goat serum, 0.1% Tween in PBS) at room temperature for 30 minutes, followed by incubation with Alexa Fluor 594-conjugated anti-BrdU antibody (Invitrogen, #B35132) solution (1:50 in blocking solution) at 4°C overnight in a humid atmosphere. The sections were rinsed in PBS, counterstained with Hoechst and mounted with anti-fade mounting gel. Images were obtained by using a Zeiss fluorescence microscope and analyzed with Imaris software. The numbers of BrdU-labeled nuclei and total nuclei were recorded for two independent control and mutant littermate pairs. The cell proliferation data were recorded and analyzed separately for the anterior and posterior regions of the palatal shelves, with data from 15-20 sections from each region of each palatal shelf. Student's *t*-test was used to analyze the differences in the datasets and $P<0.01$ was considered statistically significant.

Real-time RT-PCR
Palatal shelves were micro-dissected from E12.5 and E13.5 embryos, quickly frozen in liquid nitrogen and stored individually at −80°C. Following identification of the genotypes by allele-specific PCR, two pairs of palatal shelf samples were pooled by genotype. Total RNA was extracted using the RNeasy Micro Kit (Qiagen). First-strand cDNA synthesis was achieved using the SuperScript First-Strand Synthesis System (Invitrogen). Quantitative PCR amplifications were performed in a C1000 Touch Thermal Cycler (Bio-Rad) using the SYBR Green^{ER} qPCR Supermix (Invitrogen). Gene-specific primers were: Hprt-F (5′-TGCTGGT-GAAAAGGACCTCTCG-3′) and Hprt-R (5′-CTGGCAACAT-CAACAGGACTCC-3′); Pax9-F (5′-TATTCTGCGCAACAAGATCG-3′) and Pax9-R (5′-GGTGGTGTAGGCACCTTAGC-3′); Bmp4-F (5′-GAGGGATCTTTACCGGCTCC-3′) and Bmp4-R (5′-GTTGAAGAG-GAAACGAAAAGCAG-3′); Msx1-F (5′-AAGATGCTCTGGTGAAGGC-3′) and Msx1-R (5′-TGGTCTTGTTGCTTGCGTA-3′); Fgf10-F (5′-TTTGAGCCATAGAGTTTCCCC-3′) and Fgf10-R (5′-CGGGACCAA-GAATGAAGACTG-3′); Osr2-F (5′-TCTTTACACATCCCGCTTCC-3′) and Osr2-R (5′-GGAAAGGTCATGAGGTCCAA-3′). For each sample, the relative levels of target mRNAs were normalized to that of HPRT using the standard curve method. Four sets of samples were analyzed for each gene. Student's *t*-test was used to analyze the difference and $P<0.05$ was considered statistically significant.

References

Alappat, S. R., Zhang, Z., Suzuki, K., Zhang, X., Liu, H., Jiang, R., Yamada, G. and Chen, Y. (2005). The cellular and molecular etiology of the cleft secondary palate in Fgf10 mutant mice. *Dev. Biol.* **277**, 102-113.

Baek, J. A., Lan, Y., Liu, H., Maltby, K. M., Mishina, Y. and Jiang, R. (2011). Bmpr1a signaling plays critical roles in palatal shelf growth and palatal bone formation. *Dev. Biol.* **350**, 520-531.

Barlow, A. J., Bogardi, J. P., Ladher, R. and Francis-West, P. H. (1999). Expression of chick Barx-1 and its differential regulation by FGF-8 and BMP signaling in the maxillary primordia. *Dev. Dyn.* **214**, 291-302.

Barrow, J. R., Stadler, H. S. and Capecchi, M. R. (2000). Roles of Hoxa1 and Hoxa2 in patterning the early hindbrain of the mouse. *Development* **127**, 933-944.

Bush, J. O. and Jiang, R. (2012). Palatogenesis: morphogenetic and molecular mechanisms of secondary palate development. *Development* **139**, 231-243.

Coulter, D. E. and Wieschaus, E. (1988). Gene activities and segmental patterning in Drosophila: analysis of odd-skipped and pair-rule double mutants. *Genes Dev.* **2**, 1812-1823.

Danielian, P. S., Muccino, D., Rowitch, D. H., Michael, S. K. and McMahon, A. P. (1998). Modification of gene activity in mouse embryos in utero by a tamoxifen-inducible form of Cre recombinase. *Curr. Biol.* **8**, 1323-1326.

Dudas, M., Sridurongrit, S., Nagy, A., Okazaki, K. and Kaartinen, V. (2004). Craniofacial defects in mice lacking BMP type I receptor Alk2 in neural crest cells. *Mech. Dev.* **121**, 173-182.

Ferguson, M. W. (1988). Palate development. *Development* **103** Suppl., 41-60.

Gendron-Maguire, M., Mallo, M., Zhang, M. and Gridley, T. (1993). Hoxa-2 mutant mice exhibit homeotic transformation of skeletal elements derived from cranial neural crest. *Cell* **75**, 1317-1331.

Green, R. B., Hatini, V., Johansen, K. A., Liu, X. J. and Lengyel, J. A. (2002). Drumstick is a zinc finger protein that antagonizes Lines to control patterning and morphogenesis of the Drosophila hindgut. *Development* **129**, 3645-3656.

Gritli-Linde, A. (2007). Molecular control of secondary palate development. *Dev. Biol.* **301**, 309-326.

Hao, I., Green, R. B., Dunaevsky, O., Lengyel, J. A. and Rauskolb, C. (2003). The odd-skipped family of zinc finger genes promotes Drosophila leg segmentation. *Dev. Biol.* **263**, 282-295.

Hart, M. C., Wang, L. and Coulter, D. E. (1996). Comparison of the structure and expression of odd-skipped and two related genes that encode a new family of zinc finger proteins in Drosophila. *Genetics* **144**, 171-182.

Hilliard, S. A., Yu, L., Gu, S., Zhang, Z. and Chen, Y. P. (2005). Regional regulation of palatal growth and patterning along the anterior-posterior axis in mice. *J. Anat.* **207**, 655-667.

Ito, Y., Yeo, J. Y., Chytil, A., Han, J., Bringas, P., Jr, Nakajima, A., Shuler, C. F., Moses, H. L. and Chai, Y. (2003). Conditional inactivation of Tgfbr2 in cranial neural crest causes cleft palate and calvaria defects. *Development* **130**, 5269-5280.

Jia, S., Zhou, J., Gao, Y., Baek, J. A., Martin, J. F., Lan, Y. and Jiang, R. (2013). Roles of Bmp4 during tooth morphogenesis and sequential tooth formation. *Development* **140**, 423-432.

Lan, Y. and Jiang, R. (2009). Sonic hedgehog signaling regulates reciprocal epithelial-mesenchymal interactions controlling palatal outgrowth. *Development* **136**, 1387-1396.

Lan, Y., Kingsley, P. D., Cho, E. S. and Jiang, R. (2001). Osr2, a new mouse gene related to Drosophila odd-skipped, exhibits dynamic expression patterns during craniofacial, limb, and kidney development. *Mech. Dev.* **107**, 175-179.

Lan, Y., Ovitt, C. E., Cho, E. S., Maltby, K. M., Wang, Q. and Jiang, R. (2004). Odd-skipped related 2 (Osr2) encodes a key intrinsic regulator of secondary palate growth and morphogenesis. *Development* **131**, 3207-3216.

Levi, G., Mantero, S., Barbieri, O., Cantatore, D., Paleari, L., Beverdam, A., Genova, F., Robert, B. and Merlo, G. R. (2006). Msx1 and Dlx5 act independently in development of craniofacial skeleton, but converge on the regulation of Bmp signaling in palate formation. *Mech. Dev.* **123**, 3-16.

Li, Q. and Ding, J. (2007). Gene expression analysis reveals that formation of the mouse anterior secondary palate involves recruitment of cells from the posterior side. *Int. J. Dev. Biol.* **51**, 167-172.

Liu, W., Lan, Y., Pauws, E., Meester-Smoor, M. A., Stanier, P., Zwarthoff, E. C. and Jiang, R. (2008). The Mn1 transcription factor acts upstream of Tbx22 and preferentially regulates posterior palate growth in mice. *Development* **135**, 3959-3968.

Murray, S. A., Oram, K. F. and Gridley, T. (2007). Multiple functions of Snail family genes during palate development in mice. *Development* **134**, 1789-1797.

Ogawa, T., Kapadia, H., Feng, J. Q., Raghow, R., Peters, H. and D'Souza, R. N. (2006). Functional consequences of interactions between Pax9 and Msx1 genes in normal and abnormal tooth development. *J. Biol. Chem.* **281**, 18363-18369.

Pantalacci, S., Prochazka, J., Martin, A., Rothova, M., Lambert, A., Bernard, L., Charles, C., Viriot, L., Peterkova, R. and Laudet, V. (2008). Patterning of palatal rugae through sequential addition reveals an anterior/posterior boundary in palatal development. *BMC Dev. Biol.* **8**, 116.

Peters, H., Neubüser, A., Kratochwil, K. and Balling, R. (1998). Pax9-deficient mice lack pharyngeal pouch derivatives and teeth and exhibit craniofacial and limb abnormalities. *Genes Dev.* **12**, 2735-2747.

Rice, R., Spencer-Dene, B., Connor, E. C., Gritli-Linde, A., McMahon, A. P., Dickson, C., Thesleff, I. and Rice, D. P. (2004). Disruption of Fgf10/Fgfr2b-coordinated epithelial-mesenchymal interactions causes cleft palate. *J. Clin. Invest.* **113**, 1692-1700.

Rice, R., Connor, E. and Rice, D. P. (2006). Expression patterns of Hedgehog signalling pathway members during mouse palate development. *Gene Expr. Patterns* **6**, 206-212.

Saulier-Le Dréan, B., Nasiadka, A., Dong, J. and Krause, H. M. (1998). Dynamic changes in the functions of Odd-skipped during early Drosophila embryogenesis. *Development* **125**, 4851-4861.

Stapleton, P., Weith, A., Urbánek, P., Kozmik, Z. and Busslinger, M. (1993). Chromosomal localization of seven PAX genes and cloning of a novel family member, PAX-9. *Nat. Genet.* **3**, 292-298.

Wang, L. and Coulter, D. E. (1996). bowel, an odd-skipped homolog, functions in the terminal pathway during Drosophila embryogenesis. *EMBO J.* **15**, 3182-3196.

Wang, T., Tamakoshi, T., Uezato, T., Shu, F., Kanzaki-Kato, N., Fu, Y., Koseki, H., Yoshida, N., Sugiyama, T. and Miura, N. (2003). Forkhead transcription factor Foxf2 (LUN)-deficient mice exhibit abnormal development of secondary palate. *Dev. Biol.* **259**, 83-94.

Welsh, I. C. and O'Brien, T. P. (2009). Signaling integration in the rugae growth zone directs sequential SHH signaling center formation during the rostral outgrowth of the palate. *Dev. Biol.* **336**, 53-67.

Yu, L., Gu, S., Alappat, S., Song, Y., Yan, M., Zhang, X., Zhang, G., Jiang, Y., Zhang, Z., Zhang, Y. et al. (2005). Shox2-deficient mice exhibit a rare type of incomplete clefting of the secondary palate. *Development* **132**, 4397-4406.

Zhang, Y., Zhao, X., Hu, Y., St Amand, T., Zhang, M., Ramamurthy, R., Qiu, M. and Chen, Y. (1999). Msx1 is required for the induction of Patched by Sonic hedgehog in the mammalian tooth germ. *Dev. Dyn.* **215**, 45-53.

Zhang, Z., Song, Y., Zhao, X., Zhang, X., Fermin, C. and Chen, Y. (2002). Rescue of cleft palate in Msx1-deficient mice by transgenic Bmp4 reveals a network of BMP and Shh signaling in the regulation of mammalian palatogenesis. *Development* **129**, 4135-4146.

Zhang, Z., Lan, Y., Chai, Y. and Jiang, R. (2009). Antagonistic actions of Msx1 and Osr2 pattern mammalian teeth into a single row. *Science* **323**, 1232-1234.

Zhou, J., Gao, Y., Zhang, Z., Zhang, Y., Maltby, K. M., Liu, Z., Lan, Y. and Jiang, R. (2011). Osr2 acts downstream of Pax9 and interacts with both Msx1 and Pax9 to pattern the tooth developmental field. *Dev. Biol.* **353**, 344-353.

DEVELOPMENT